Journal of Theoretical Biology 263 (2010) 407–418

Contents lists available at ScienceDirect

Journal of Theoretical Biology

journal homepage: www.elsevier.com/locate/yjtbi

A macroscopic ansatz to deduce the Hill relation

Michael Günther [a,b,c,*], Syn Schmitt [d]

[a] Eberhard–Karls–Universität, Institut für Sportwissenschaft, Arbeitsbereich III, Wilhelmstraße 124, D-72074 Tübingen, Deutschland, Germany
[b] Friedrich–Schiller–Universität, Institut für Sportwissenschaft, Lehrstuhl für Bewegungswissenschaft, Seidelstraße 20, D-07749 Jena, Deutschland, Germany
[c] Eberhard–Karls–Universität, Orthopädische Klink, Biomechaniklabor, Hoppe–Seyler–Straße 3, D-72076 Tübingen, Deutschland, Germany
[d] Universität Stuttgart, Institut für Sport- und Bewegungswissenschaft, Allmandring 28, D-70569 Stuttgart, Deutschland, Germany

ARTICLE INFO

Article history:
Received 1 November 2008
Received in revised form
23 December 2009
Accepted 24 December 2009
Available online 4 January 2010

Keywords:
Hill equation
Muscle model
Contraction dynamics
Biomechanics

ABSTRACT

In this study, we derive the hyperbolic force–velocity relation of concentric muscular contraction, first formulated empirically by A.V. Hill in 1938, from three essential model assumptions: (1) the structural assembly of three well-known elements – i.e. active, parallel damping, and serial – fulfilling a force equilibrium, (2) the parallel damping coefficient explicitly depending on muscle force output and three parameters, and (3) the kinematic gearing ratio between active and serial element being assigned to a parameter. The energy source within the muscle represented by the force of the active element is an additional fifth parameter. As a result we find the Hill "constants" A and B as functions of our five model parameters. Using A and B values from literature on experimental data, we predict heat power release of our model. By calculating enthalpy rate and mechanical efficiency, we compare the model heat power to predictions from another Hill-type model, to Hill's original findings, and to findings from modern muscle heat measurements. We reconsider why the biggest share of heat rate during isometric contractions (maintenance heat) and the velocity-dependent heat rate during concentric contractions in addition to maintenance heat rate (shortening heat rate) may be traced back to the same mechanism represented by the kinematic gearing ratio. Namely, we suggest that the serial element transfers attachment–detachment fluctuations of actin–myosin crossbridges within one sarcomere to others in the same sarcomere and to those in parallel and in series. Numerically, in case of negligible passive muscular damping, we find the ratio between A and isometric force (relative A) to depend exclusively on the kinematic gearing ratio, whereas the maintenance heat rate scales with the square of relative A. Moreover, this mechanical coupling internal to the muscle fibres may also be behind the macroscopic force dependency of the overall parallel damping coefficient.

1. Introduction

Hill (1938) published his famous paper in which he fixed the hyperbolic relation between muscular force and velocity during concentric contractions from heat measurements empirically. The isometric force is one parameter of this relation, whereas he named the two remaining parameters the "dynamic constants of muscle". Later, he acknowledged that the force–velocity relation had to be modified for a better reproduction of the decrease in enthalpy rate found at high shortening velocities (Hill, 1964). Still, a hyperbolic relation remained with now five parameters necessary to align with experimental findings.

Huxley (1957) presented the first comprehensive theoretical model, based on the "sliding filament theory". He derived the known force–velocity relation of a muscle (Hill, 1938) from mapping the state of the art knowledge about the structure of the crucial molecules involved in the crossbridge cycling mechanism of muscular force production. He needed to set nine microscopic parameters in order to fit the Hill (1938) relation. Assuming a two-stage cycle, a later refinement of Huxley's (1973) sliding filament model again succeeded in reproducing the enthalpy rate factored in by Hill's (1964) modification. The number of sliding filament model parameters remained the same.

When talking about models, we will label them in the following as either "Hill-type" or "Huxley-type". The latter denomination gains somehow double weight as Hugh Esmor Huxley and Jean Hanson (Hanson and Huxley, 1953; Huxley and Hanson, 1954) were on their way to put forward the sliding filament model simultaneously (Huxley, 2004, 2008) to Andrew Fielding Huxley and Ralph Niedergerke (Huxley and Niedergerke, 1953).

The empirically derived Hill relation is not self-explanatory. For example, it might constitute a thermodynamical state equation or a fairly complex visco-elastic force law. In numerical neuro-musculo-skeletal model simulations Hill-type models are usually used in the force law sense (Günther and Ruder, 2003;

* Corresponding author at: Eberhard–Karls–Universität, Institut für Sportwissenschaft, Arbeitsbereich III, Wilhelmstraße 124, D-72074 Tübingen, Deutschland, Germany. Tel.: +49 7071 2976041.
E-mail address: s7gumi@uni-jena.de (M. Günther).

0022-5193/$ - see front matter © 2010 Elsevier Ltd. All rights reserved.
doi:10.1016/j.jtbi.2009.12.027

Nomenclature

List of symbols, terms, and definitions

SE	serial element
AE	active element
PDE	parallel damping element
l_M	length of the muscle
$\dot{l}_M$	contraction velocity of the muscle
l_{SE}	length of the SE (internal degree of freedom)
$\dot{l}_{SE}$	contraction velocity of the SE
κ_v	$=\dot{l}_{SE}/\dot{l}_M$; gearing ratio of internal to external contraction velocity
l_{AE}	$=l_M-l_{SE}=l_{PDE}$; length of the AE (and PDE)
$\dot{l}_{AE}$	$=\dot{l}_M-\dot{l}_{SE}=\dot{l}_{PDE}$; contraction velocity of the AE (and PDE)
q	normalised muscle activation
F_M	force generated by the muscle
$F_{M,0}$	isometric ($\dot{l}_M=0$) force of the muscle
F_{SE}	$=F_M$; force of the SE
F_{AE}	force of the AE
F_{PDE}	force of the PDE
$F_{AE,max}$	maximum force of the AE
A	Hill parameter: asymptote $F_M(\dot{l}_M)=-A$, i.e. parallel to velocity-axis
B	Hill parameter: asymptote $\dot{l}_M(F_M)=B$, i.e. parallel to force-axis
$\dot{l}_{M,max}$	$=B/A\cdot F_{M,0}$; absolute value of concentric contraction velocity at $F_M=0$
$A_{rel}=A/F_{M,0}$	normalised Hill parameter
$l_{CE,opt}$	optimal length of assembly of active muscle fibres (not a parameter in our model; literature data)
$B_{rel}=B/l_{CE,opt}$	normalised Hill parameter
$d_{PDE}(F_M)$	damping coefficient of the PDE linearly depending on F_M
$D_{PDE,max}$	maximum value of $d_{PDE}(F_M)$
R_{PDE}	minimum value of $d_{PDE}(F_M)$ normalised to $D_{PDE,max}$
$\dot{h}$	shortening heat rate
$\dot{h}_0$	maintenance heat rate
$c_{\dot{h}_0}(T-T_0,params)$	temperature (and other parameters) dependent factor of $\dot{h}_0$
T	temperature (reference value T_0)
$\dot{\mathcal{H}}=-F_M\cdot\dot{l}_M+\dot{h}+\dot{h}_0$	enthalpy rate of the muscle
$\varepsilon_M=-F_M\cdot\dot{l}_M/\dot{\mathcal{H}}$	mechanical efficiency of the muscle

Günther et al., 2007; Houdijk et al., 2006; Kistemaker et al., 2006; van Soest and Bobbert, 1993) interpreting it uni-directionally, with the force given and the respective velocity constituting the model response. As real muscle can respond to different protocols demanding a variety of disturbances, including force and length steps, bi-directionality seems to be one important criterion, among others, for a predictive muscle model. Hill (1970) himself meant to read his relation bi-directionally. In contrast, to the best of our knowledge none of the Huxley-type models developed so far (Barclay, 1999; Chin et al., 2006; Cooke et al., 1994; Huxley, 1957, 1973; Lan and Sun, 2005; Piazzesi and Lombardi, 1995, 1996) can be applied bi-directionally. We have found one study (Baker and Thomas, 2000) yet, deriving contraction velocity as a hyperbolic function of force with the muscle fulfilling thermodynamic equilibrium.

Our aim is to build a bi-directional Hill-type muscle model as simple as possible, i.e. based on less parameters than Huxley-type models, and of predictive character. Thereto, the Hill relation must be derived from basic principles, either at least one independent equation or microscopic mechanisms. Concretely, we derive the Hill relation from a force equilibrium of mechanical structures rather than exclusively from an explicit model of the source of mechanical power as Huxley (1957, 1973, 2000) did following Hill's (1938) empirical path. Our model is meant to provide some insight into the mechanical behaviour of a muscle as a whole. In particular, we suggest a causal explanation for the origin of the Hill relation in terms of only three macroscopic mechanical parameters and one well-established internal degree of freedom which is resolved by a gearing ratio between internal and external contraction. Consequently, the model can be used to predict the force–velocity relationship for muscle with given architectural parameters, rather than having to measure the force–velocity relationship directly.

2. Methods

Our model coarsely maps the macroscopic features of an assembly of active muscle fibres incorporating three basic, physiologically motivated, structural elements (Fig. 1). In the following we will derive the Hill relation from one basic equation and two additional features. First, the serial arrangement of model elements implies the introduction of one degree of freedom, representing an internal length measure that occurs in addition to the length of the active muscle fibres. This is dealt with by applying a kinematic gearing ratio between the elements in series. Second, a simple force law for the parallel damper is assumed. The characteristics of the other two elements do not have to be specified.

The first element is the source, and possibly drain, of mechanical energy. It is called the active element (AE) producing the force F_{AE}. In macroscopic muscle models the chemical state, i.e. the relative number of actively force-producing crossbridges, can be quantified by normalised muscle activation $0\le q\le 1$. The naming of any further model element is chosen due to its functional role with respect to the AE.

The second element is the serial element (SE) loaded with the force F_{SE}. It maps compliant structures within the muscle fibres (Hill, 1938, 1950; Katz, 1939; Krueger and Pollack, 1975; Kishino and Yanagida, 1988; Levin and Wyman, 1927; Lindstedt et al., 2002; Maruyama et al., 1977; Neumann et al., 1998; Pandy et al.,

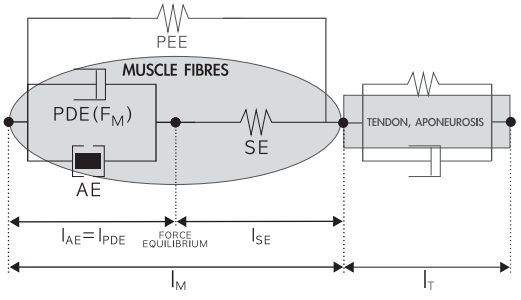

Fig. 1. The macroscopic model of the muscle consisting of the active (AE), parallel damping (PDE), and serial (SE) element. Not being part of the model, parallel elastic element (PEE), tendon, and aponeurosis are depicted additionally (greyed element symbols). The term "muscle" denotes the arrangement of all activatable muscle fibres. The damping coefficient of the PDE depends linearly on muscle force F_M (Eq. (4)) which in turn both equates (force equilibrium) the force in the SE and the sum of the forces of AE plus PDE (Eq. (2)). The muscle length is l_M and the internal length degree of freedom is represented by l_{SE}.

1990; Wakabayashi et al., 1994; Zajac, 1989). A recent approach (Denoth et al., 2002; Telley and Denoth, 2007), modelling the muscle as an inhomogeneous chain of many force generators coupled visco-elastically to each other both in parallel and in series, incorporates series elasticity as a key feature.

The third element is the parallel damping element (PDE) producing a frictional force F_{PDE}. Energy dissipation within the muscle can be a passive (Günther et al., 2007; Minajeva et al., 2001; Wang et al., 1993) or an active (Gasser and Hill, 1924; Hartree and Hill, 1920; Hill, 1922; Levin and Wyman, 1927; Lupton, 1922, 1923) phenomenon. Two studies point to a dependency of the PDE on muscle force (Baker and Thomas, 2000; Pate and Cooke, 1991).

The kinematic relation for the lengths of the elements AE, PDE on the one hand and the SE on the other hand, arranged in series, writes

$$l_{AE} = l_{PDE} = l_M - l_{SE} \tag{1}$$

with l_M representing the muscle length (Fig. 1). The basic equation describing the mechanics of our muscle model is the equilibrium of the forces generated by the elements AE, PDE, and SE

$$F_M = F_{SE} = F_{AE} + F_{PDE} \tag{2}$$

with

$$F_{PDE} = d_{PDE} \cdot \dot{l}_{PDE} = d_{PDE} \cdot (\dot{l}_M - \dot{l}_{SE}), \tag{3}$$

whereat we took the first time derivative (dot symbol " $\dot{}$ ") of Eq. (1) into account. The PDE is the only element within this study to which we attribute a specific functional dependency. We assume that its force depends linearly on the contraction velocity $\dot{l}_{AE}$ of the AE (see Eq. (3)) and a respective damping coefficient

$$d_{PDE}(F_M) = D_{PDE,max} \cdot \left((1 - R_{PDE}) \cdot \frac{F_M}{F_{AE,max}} + R_{PDE} \right) \tag{4}$$

depending linearly on the current force F_M of the muscle which equates the force in the SE (Eq. (2)), whereat $D_{PDE,max}$ is the maximum $d_{PDE}(F_M)$ value (at $F_M = F_{AE,max}$ with conceiving of $F_{AE,max}$ as maximum isometric force) and R_{PDE} is the minimum $d_{PDE}(F_M)$ value (passive damping in an inactive muscle) normalised to $D_{PDE,max}$. Note that this force-dependency of d_{PDE} is the only non-linearity that we introduce explicitly into our model.

Furthermore, by defining the isometric ($\dot{l}_M = 0$) muscle force as

$$F_{M,0} = F_M(\dot{l}_M = 0), \tag{5}$$

by working out the force equilibrium (Eq. (2)) in the isometric condition, with F_{PDE} substituted by Eq. (3), next solving the equilibrium in isometry for

$$F_{AE} = F_{M,0} + d_{PDE}(F_{M,0}) \cdot \dot{l}_{SE}, \tag{6}$$

and finally re-substituting Eq. (6) into the general force equilibrium (Eq. (2)) we find

$$F_M = F_{M,0} + d_{PDE}(F_{M,0}) \cdot \dot{l}_{SE} + d_{PDE}(F_M) \cdot (\dot{l}_M - \dot{l}_{SE}). \tag{7}$$

In a nutshell, we reduced the manifold of all possible solutions of Eq. (2) for the relation between $\dot{l}_M$ and F_M to those with one specific value of the isometric force $F_{M,0}$ as defined by Eq. (5). Thus, $F_{M,0}$ is used as a parameter here. For a chosen isometric muscle force value $F_{M,0}$ the related force F_{AE} acting in the AE, and vice versa according to (Eq. (6)), is potentially a function of internal length re-distribution $\dot{l}_{SE}$.

We aim at relating the muscle force F_M explicitly to muscle contraction velocity $\dot{l}_M$. With this in mind, Eq. (7) is a preliminary result, because F_M still depends explicitly on both the external muscle contraction velocity $\dot{l}_M$ and the contraction velocity of the internal degree of freedom $\dot{l}_{SE}$. By assuming that a gearing ratio

$$\kappa_v = \frac{\dot{l}_{SE}}{\dot{l}_M} \tag{8}$$

between internal and external velocity can be specified, the force equilibrium as manifested by Eq. (7) transforms to

$$(F_M - F_{M,0}) - \dot{l}_M \cdot (d_{PDE}(F_M) \cdot (1 - \kappa_v) + d_{PDE}(F_{M,0}) \cdot \kappa_v) = 0 \tag{9}$$

which is an equation relating $\dot{l}_M$ to F_M. In Appendix A we suggest what κ_v might depend on. Eq. (9) is the force equilibrium expressed in Eq. (2) with the current distribution between $\dot{l}_{SE}$ and $\dot{l}_{AE}$ specifically expressed by one parameter κ_v, while $F_{M,0}$ represents another one.

There is no physical reason to favour either $\dot{l}_M$ or F_M as the independent variable within Eq. (9). The idea that muscle force and velocity are interchangeable as dependent and independent variables is a generally understood principle and in accordance with Hill's (1970) view. So far, this idea is not often applied in muscle modelling. At least in our approach, we may solve Eq. (9) either for $F_M = F_M(\dot{l}_M)$ or for $\dot{l}_M = \dot{l}_M(F_M)$, whenever appropriate. Eq. (9) is a bi-directional relation. Transformation between both views is uniquely determined if d_{PDE} is a linear function of F_M as assumed here (Eq. (4) with $F_M = F_{SE}$). In this case, Eq. (9) constitutes a hyperbola

$$(F_M + A) \cdot \dot{l}_M = -B \cdot (F_{M,0} - F_M) \tag{10}$$

with the parameters A, B, $F_{M,0}$ being positive and $\dot{l}_M$ consistently being negative in the shortening (concentric) case.

The numbers A, B, $F_{M,0}$ are functions of our five model parameters. This becomes clear by comparing the terms in the Hill relation equation (10) solved for the contraction velocity $\dot{l}_M = B \cdot (F_M - F_{M,0})/(F_M + A)$ to Eq. (9) solved for

$$\dot{l}_M = \frac{F_M - F_{M,0}}{(1 - \kappa_v) \cdot d_{PDE}(F_M) + \kappa_v \cdot d_{PDE}(F_{M,0})} \tag{11}$$

which becomes

$$\dot{l}_M = \frac{1}{\frac{D_{PDE,max}}{F_{AE,max}} \cdot (1 - R_{PDE})} \cdot \frac{F_M - F_{M,0}}{(1 - \kappa_v) \cdot F_M + \frac{R_{PDE}}{(1 - R_{PDE})} \cdot F_{AE,max} + \kappa_v \cdot F_{M,0}} \tag{12}$$

expressed explicitly in terms of our model parameters. Thereto, the linear transforming operations

$$d_{PDE}(x_1 - x_2) = d_{PDE}(x_1) - d_{PDE}(x_2) + D_{PDE,max} \cdot R_{PDE},$$

$$d_{PDE}(x_1 - x_0) - d_{PDE}(x_2 - x_0) = d_{PDE}(x_1) - d_{PDE}(x_2),$$

must be used for $d_{PDE}(F_M)$ after Eq. (4).

Finally, the Hill parameters emerge as explicit functions of our model parameters

$$A = \frac{R_{PDE}}{(1 - R_{PDE}) \cdot (1 - \kappa_v)} \cdot F_{AE,max} + \frac{\kappa_v}{1 - \kappa_v} \cdot F_{M,0}, \tag{13}$$

$$B = \frac{1}{\frac{D_{PDE,max}}{F_{AE,max}} \cdot (1 - R_{PDE}) \cdot (1 - \kappa_v)}. \tag{14}$$

Accordingly, the maximum shortening velocity writes

$$\dot{l}_{M,max} = \frac{B}{A} \cdot F_{M,0} = \frac{F_{AE,max}}{D_{PDE,max}} \cdot \frac{F_{M,0}}{\kappa_v \cdot (1 - R_{PDE}) \cdot F_{M,0} + R_{PDE} \cdot F_{AE,max}}. \tag{15}$$

The unloaded muscle ($F_M = 0$) would contract concentrically with $\dot{l}_M = -\dot{l}_{M,max}$.

In the limit case of neglected minimum (passive) internal parallel damping ($R_{PDE} = 0$) the Hill parameters arise from

Eqs. (13) and (14) as

$$A = \frac{\kappa_v}{1-\kappa_v} \cdot F_{M,0}, \tag{16}$$

$$B = \frac{F_{AE,max}}{(1-\kappa_v) \cdot D_{PDE,max}} = \frac{\kappa_v}{1-\kappa_v} \cdot \dot{l}_{M,max}, \tag{17}$$

with the maximum shortening velocity (compare Eq. (15))

$$\dot{l}_{M,max} = \frac{F_{AE,max}}{\kappa_v \cdot D_{PDE,max}}. \tag{18}$$

Note that a concurrent parameter variation fulfilling $B/A = const.$ meets the constraint $\dot{l}_{M,max} = const.$, whereat solely the curvature is changed. In our model this is equivalent to $\kappa_v \cdot D_{PDE,max} = const.$

From hereon, we will think of the hyperbolic equation (10) as $\dot{l}_M = \dot{l}_M(F_M)$, naming it the "Hill relation". The emergence of the Hill relation $\dot{l}_M(F_M)$, according to the two velocity-dependent terms in Eqs. (7) and (9) and the specific function equation (4), might become more transparent by being explained graphically (see Appendix B). In total, we have introduced five parameters, four of which ($F_{M,0}, \kappa_v, D_{PDE,max}, F_{AE,max}$) essentially forming the hyperbola and one (R_{PDE}) being an optional modifier.

The concentric contraction velocity v was a positive number in the original formulation of the Hill (1938) relation

$$(P+a) \cdot v = b \cdot (P_0 - P). \tag{19}$$

Thus, a comparison to Eq. (10) gives $v = -\dot{l}_M$, $P = F_M$, $P_0 = F_{M,0}$, $a = A$, $b = B$.

3. Results

Empirically, both mechanics and heat release during concentric muscle contractions are represented by all three parameters of the Hill relation. Therefore, we choose appropriate parameters in accordance with literature data first. Second, in order to validate our model generally, its predicted mechanical and heat power are compared to force–velocity and enthalpy rate measurements. Third, the model allows for an estimation of the mechanical power distribution between AE, PDE, and SE.

3.1. An estimate of model parameters

A median piglet muscle (Günther et al., 2007) would be represented by $F_{M,0} = F_{AE,max} = 30\,\mathrm{N}$, $\kappa_v = 0.2$, $D_{PDE,max} = 1000\,\mathrm{N\,s/m}$ (i.e. $\dot{l}_{M,max}|_{R_{PDE}=0} = 0.15\,\mathrm{m/s}$, $A_{rel}|_{R_{PDE}=0} = 1/4$), and $R_{PDE} = 0.01$ (i.e. $\dot{l}_{M,max}|_{R_{PDE}=0.01} = 0.144\,\mathrm{m/s}$). On the one hand, this muscle can be compared to more recent experimental findings (Barclay et al., 1993; Curtin and Woledge, 1993; Barclay, 1994, 1996). On the other hand, the κ_v,A_{rel} choice (see Eqs. (13) and (16)) accords with Hill's (1938) original and later (Hill, 1964) work. In order to validate our model, we follow the same path as a recent computer simulation study (Houdijk et al., 2006) in which the muscular enthalpy rate along with the mechanical efficiency was predicted by modelling muscular heat rates as functions of the AE state variables q, l_{AE} during isovelocity contractions, while assuming a fully activated muscle ($q = 1$).

3.2. Maintenance heat rate, enthalpy rate, mechanical efficiency: a model validation

The PDE is the only explicitly formulated element within our model (Eq. (4)). Thus, we can calculate the minimum dissipative loss $\dot{h} = d_{PDE}(F_M) \cdot \dot{l}_{AE}^2 = d_{PDE}(F_M) \cdot ((1-\kappa_v) \cdot \dot{l}_M)^2$ during a concentric contraction. With that, we can predict the enthalpy rate

$$\dot{\mathcal{H}} = -F_M \cdot \dot{l}_M + \dot{h} + \dot{h}_0, \tag{20}$$

knowing the contraction velocity $\dot{l}_M$ from Eq. (11) or (12), respectively. The first term is the net mechanical power output of the muscle, the second term $\dot{h}$ is its shortening heat rate, and the third term $\dot{h}_0$ is its maintenance heat rate. The latter is an unavoidable energy loss owing to the fact that an active muscle, loaded isometrically, produces heat at the rate $\dot{h}_0$ due to crossbridge cycling, even though it does not do any mechanical work at all. Taking these three terms into account, the assumed enthalpy rate $\dot{\mathcal{H}}$ (Eq. (20)) is the theoretical minimum power the muscle has to generate to gain its net mechanical power output.

This is equivalent to assuming that all other hypothetical internal elements work without loss and no other heat generating process does exist. For example, in order to keep the model as simple as possible, we neglected the activation heat, released due to any Ca^{2+}–flux into and out of the sarcoplasmatic reticulum as a response to stimulation – also called excitation – from action potentials. Whereas maintenance heat primarily depends on filament overlap and free Ca^{2+}–concentration (state of activation q), activation heat depends on stimulation frequency. Maximum activation heat rate is roughly half as high as maintenance heat rate (Barclay et al., 2007; Houdijk et al., 2006). Therefore, the heat contributions to enthalpy rate $\dot{\mathcal{H}}$ are systematically underestimated within this study, while the mechanical efficiency as defined by the ratio

$$\varepsilon_M = \frac{-F_M \cdot \dot{l}_M}{\dot{\mathcal{H}}} \tag{21}$$

is over-estimated.

As part of the enthalpy rate the maintenance heat rate $\dot{h}_0$ must be known. According to literature, which indicates diverse findings about maintenance heat rate in various muscle preparations, the maintenance heat rate $\dot{h}_0$ may generally be rather proportional to than equal to $A \cdot B$ ($= 1/16 \cdot F_{M,0} \cdot \dot{l}_{M,max}$ if $A = 1/4 \cdot F_{M,0}$). Thus, in the first instance, we assume phenomenologically

$$\dot{h}_0 = c_{\dot{h}_0}(T - T_0, params) \cdot F_{M,0}(T = T_0, params) \cdot \dot{l}_{M,max}(T = T_0, params) \tag{22}$$

to adopt the view that $\dot{h}_0$ runs approximately in proportion to the number of currently active crossbridges (Houdijk et al., 2006). This implies, as a first guess, that $\dot{h}_0$ scales with [$overlap \cdot activated\ volume/time = overlap \cdot activation \cdot cross\ \ sectional$ area $\cdot\ length/time$], therefore with the product $F_{M,0} \cdot \dot{l}_{M,max}$. Additionally, $\dot{h}_0$ should increase with temperature T, while T_0 means a reference temperature. This and other dependencies – not explicitly modelled here ($params$) – are represented by the coefficient $c_{\dot{h}_0}(T - T_0, params)$.

In Hill's (1938) original experiments on frog sartorius muscle at $T = 0\,^{\circ}\mathrm{C}$ approximate numerical equality $\dot{h}_0 = A \cdot B$ was found, which was also exactly implied by Huxley in order to fit his muscle model to the Hill relation (Huxley, 1957, 1973). There is another, pure mathematical, argument (McMahon, 1984) in favour of $\dot{h}_0 = A \cdot B$. For the addition of $A \cdot B$ to both sides of Eq. (10) or (19) provides an immediate transformation of the Hill relation to the force–velocity relation derived earlier from mere mechanical measurements (Fenn and Marsh, 1935). Later modifications of the hyperbolic $\dot{l}_M(F_M)$ relation introduced by Hill (1964) himself demonstrate that the Hill parameter A may incorporate two different heat portions, one depending on load and one on velocity. Thus, the product $A \cdot B$

is somehow unlikely to be exactly equal to the heat rate at zero velocity.

Yet, by accepting $\dot{h}_0 = A \cdot B$ for a start, utilising the approximation $R_{PDE} = 0$, and comparing Eqs. (16)–(18) to (22), we predict

$$c_{\dot{h}_0} = (\kappa_v/(1-\kappa_v))^2. \tag{23}$$

The lowest and highest $c_{\dot{h}_0}$ values (0.01, 0.3) extracted from literature (Barclay, 1994, 1996; Barclay et al., 1993; Elzinga et al., 1987; Günther et al., 2007; Hill, 1938; Houdijk et al., 2006; Wank et al., 2006) correspond to $\kappa_v = 0.09, 0.35$. A median value $\kappa_v = 0.2$ corresponds to $A = A_{rel} \cdot F_{M,0} = 1/4 \cdot F_{M,0}$ (for $R_{PDE} = 0$: Eq. (16)) with the belonging factor

$$A_{rel} = \kappa_v/(1-\kappa_v). \tag{24}$$

The value $A_{rel} = 1/4$ was both originally found by Hill (1938) for a frog sartorius muscle at $T = 0\,^{\circ}$C and represents the average value of further studies (Barclay, 1994, 1996; Barclay et al., 1993; Günther et al., 2007; Houdijk et al., 2006). Eqs. (23) and (24) result in

$$c_{\dot{h}_0} = A_{rel}^2, \tag{25}$$

i.e. $A_{rel} = 1/4$, $\kappa_v = 0.2$, and $c_{\dot{h}_0} = 0.0625$ correspond to each other.

Therefore, in Fig. 2 the enthalpy rate in excess of maintenance heat rate and the mechanical efficiency predicted by this median muscle ($\kappa_v = 0.2$) can be easily compared to (i) Hill's original direct measurements of mechanical power and heat rates (Hill, 1938) and to (ii) his more accurate data published later (Hill, 1964). Additionally, we compare enthalpy rate and efficiency to (iii) the prediction of $\dot{h}$ calculated from another simple mechanical model which assumes $F_{M,0}$ to represent the energy source and in which a non-linear parallel damper is

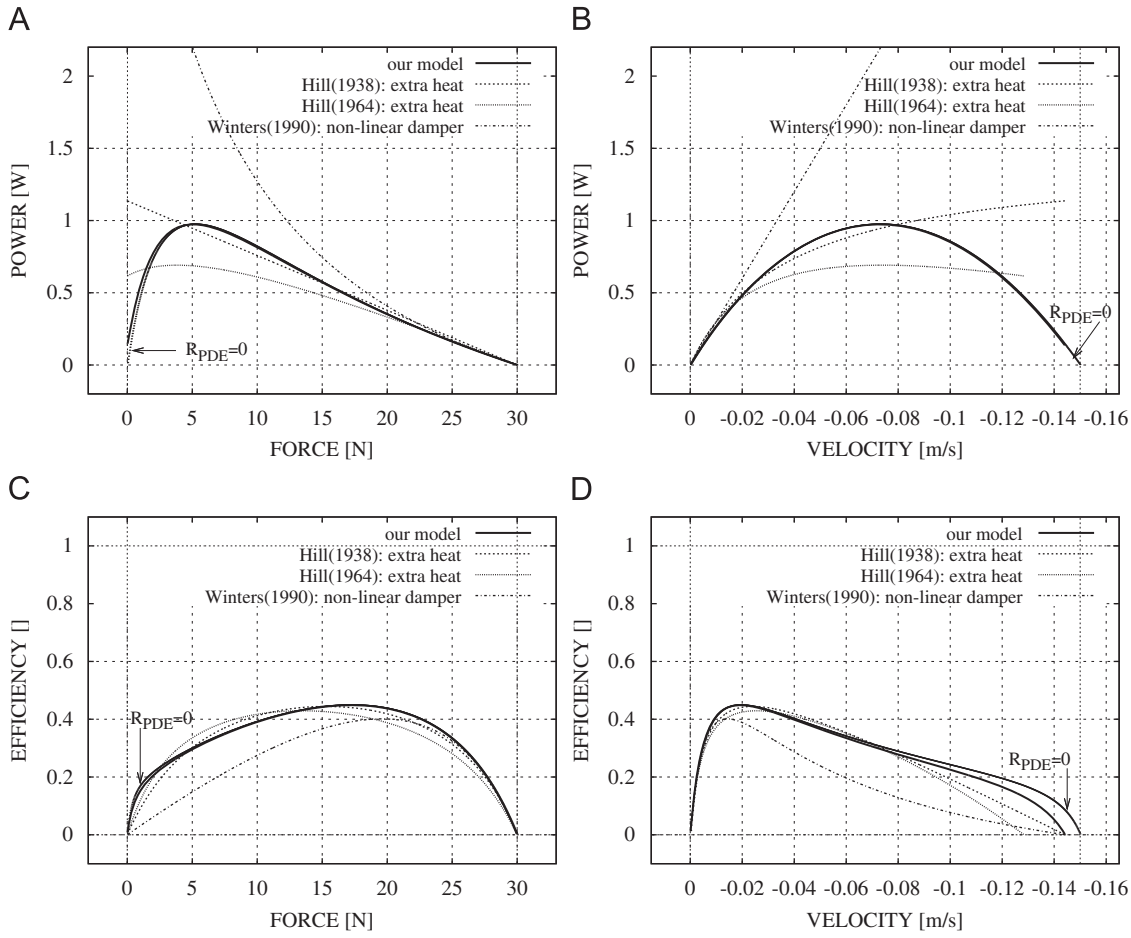

Fig. 2. (A,B) Enthalpy rate $\dot{\mathcal{H}} = -F_M \cdot \dot{l}_M + \dot{h}$, i.e. the denominator of the mechanical efficiency ε_M minus maintenance heat rate $\dot{h}_0 = 0$ (compare Eqs. (20) and (21)), as a function of (A) muscle force F_M or of (B) contraction velocity $\dot{l}_M$, for four different approaches to calculate the extra (to maintenance heat rate) energy loss per time $\dot{h}$ during contraction (shortening heat rate) either as mechanical dissipation (damping) or as "extra" heat (Hill (1938) used "extra heat" which is termed "shortening heat" here):

1. our model (solid line): $\dot{h} = (1-\kappa_v)^2 \cdot d_{PDE}(F_M) \cdot \dot{l}_M^2$,
2. "extra" heat according to Hill (1938) (dashed line): $\dot{h} = -A \cdot \dot{l}_M$ with A due to Eq. (13),
3. "extra" heat according to Hill (1964); Huxley (1973); McMahon (1984) (dotted line) with B after Eq. (14), $\alpha_{F_{M,0}} = 0.16$, $\alpha_{F_M} = 0.18$, $\gamma = 0.135$, i.e. $A' = (\alpha_{F_{M,0}} + \gamma)/(1+\alpha_{F_M}) \cdot F_{M,0}$ and $B' = B/(1+\alpha_{F_M})$,
4. non-linear damper according to Winters (1990) (dash-dotted line): $\dot{h} = -(F_{M,0}+A)/(\dot{l}_M - B) \cdot \dot{l}_M^2$.

Muscle parameters according to Section 3.1 are: $F_{M,0} = F_{AE,max} = 30$ N, $\kappa_v = 0.20$, $D_{PDE,max} = 1000$ N s/m (i.e. $\dot{l}_{M,max}|_{R_{PDE}=0} = 0.15$ m/s, $A_{rel}|_{R_{PDE}=0} = 1/4$), $R_{PDE} = 0.01$ (i.e. $\dot{l}_{M,max}|_{R_{PDE}=0.01} = 0.144$ m/s). The case $R_{PDE} = 0$ is plotted for comparison.

Our model for the case $R_{PDE} = 0.01$ (thick solid line) and, alternatively, for $R_{PDE} = 0.0$ (thin solid line: $\dot{l}_{M,max} = 0.15$ m/s). The other models: Hill (1938) with identical A and B, Hill (1964) with $A(F_M) = \alpha_{F_{M,0}} \cdot F_{M,0} + \alpha_{F_M} \cdot F_M$. The above values of $\alpha_{F_{M,0}}$, α_{F_M}, γ approximate $A = \frac{1}{4}$ (see Hill, 1964). Note that the effective B and therefore $\dot{l}_{M,max}$ are reduced. An alternative Hill-type model (pure F_{AE}, i.e. without SE which always implies $F_{AE} = F_{M,0}$) after Winters (1990) with a non-linear damper $d_M(\dot{l}_M) = (F_{M,0}+A)/(B-\dot{l}_M)$ in parallel to the force generator F_{AE} providing the same hyperbolic Hill relation as our model: $F_M(\dot{l}_M) = F_{M,0} + d_M(\dot{l}_M) \cdot \dot{l}_M$. Its enthalpy rate in excess of the maintenance heat rate is $F_{M,0} \cdot \dot{l}_M(F_M)$.

(C,D) Comparison of the respective mechanical efficiencies $\varepsilon_M = (-F_M \cdot \dot{l}_M)/(-F_M \cdot \dot{l}_M + \dot{h} + \dot{h}_0)$ for the four different models including maintenance heat rate $\dot{h}_0 = c_{\dot{h}_0} \cdot F_{M,0} \cdot \dot{l}_{M,max}$ (Eq. (22)) with $c_{\dot{h}_0} = (\kappa_v/(1-\kappa_v))^2 = A_{rel}^2 = \frac{1}{16} = 0.0625$ (according to Eqs. (16) and (17)), i.e. assuming exact equality $\dot{h}_0 = A \cdot B$.

chosen to reproduce the Hill relation exactly (Winters, 1990). Consistently, for these three comparative model cases the parameter values A, B of our median muscle are adopted (for details see legend of Fig. 2). Enthalpy rate and mechanical efficiency are both plotted versus muscle force and contraction velocity, because in some cases force-plots (compare Fig. 3) and in other cases velocity-plots (see the subtle $\dot{l}_{M,max}$ differences between both Hill-cases in Fig. 2(D)) are more case-sensitive. Moreover, either data presentations are used in literature.

Our model reasonably approximates Hill's measured enthalpy rates for $F_M > F_{M,0}/10$ (Fig. 2(A)) or $|\dot{l}_M| < 2/3 \cdot \dot{l}_{M,max}$, respectively (Fig. 2(B)). Furthermore, our model predicts a maximum in enthalpy rate which is located nearby force and velocity values also reported by Hill (1964), Huxley (1973), and another, more recent, Hill-type muscle model (Lichtwark and Wilson, 2005). However, beyond the just mentioned boundaries, an unrealistically steep decrease to almost (note: $R_{PDE} \neq 0$) maintenance heat rate is predicted for very low forces and high velocities, respectively. When taking more recent measurements into account (Fig. 4(A)), unincisive maxima in enthalpy rate may be distinguishable for some muscle preparations (Barclay et al., 1993; Barclay, 1994, 1996) or unobservable in others (Barclay et al., 1993; Curtin and Woledge, 1993; Barclay, 1996). Note, if we included activation heat into enthalpy rate (Eq. (20)) and normalised the latter to the sum of maintenance and activation heat rate, the relative enthalpy rate values as predicted in Fig. 4(A) would be about one third lower.

Generally, our model predicts enthalpy rates considerably better than the non-linear damper model (Winters, 1990) not incorporating a SE. Hereby, the discrepancies become more apparent by looking at enthalpy rate (Fig. 2(A,B)) than by looking at mechanical efficiency (Fig. 2(C,D)). The maximum deviation of measured efficiencies calculated in our model from those determined by Hill's experiments is about 10% (Fig. 2(C,D)). Almost 100% deviations, occurring for a wider range of muscle preparations (Fig. 4(B)), can be explained by variations in properties of the examined muscles, e.g. the curvature of the force–velocity relation $\dot{l}_M(F_M)$ or the course of the maintenance heat rate (Fig. 3). Note again that we slightly over-estimate efficiency due to neglecting activation heat rate.

3.3. The mechanical power output

The net mechanical power released by the muscle during a concentric contraction is $-F_M \cdot \dot{l}_M$, here defined as a positive number with a pulling force $F_M > 0$ and $\dot{l}_M < 0$ in case of shortening. Remembering Fig. 1 with $l_M = l_{AE} + l_{SE}$ (Eq. (1)) and the force equilibrium (Eq. (2); F_{PDE} corresponding to Eq. (3)) the net muscle power output rewrites $-F_M \cdot \dot{l}_M = -F_M \cdot (\dot{l}_{AE} + \dot{l}_{SE}) = -(F_{AE} + F_{PDE}) \cdot \dot{l}_{AE} - F_{SE} \cdot \dot{l}_{SE}$. Now we can infer from Eq. (8) that the relative power contribution of the SE unloading is $\kappa_v \cdot 100\%$ and the net contribution of AE plus PDE is $(1-\kappa_v) \cdot 100\%$. Therefore, our model predicts the SE to contribute $9, \ldots, 35\%$ (compare

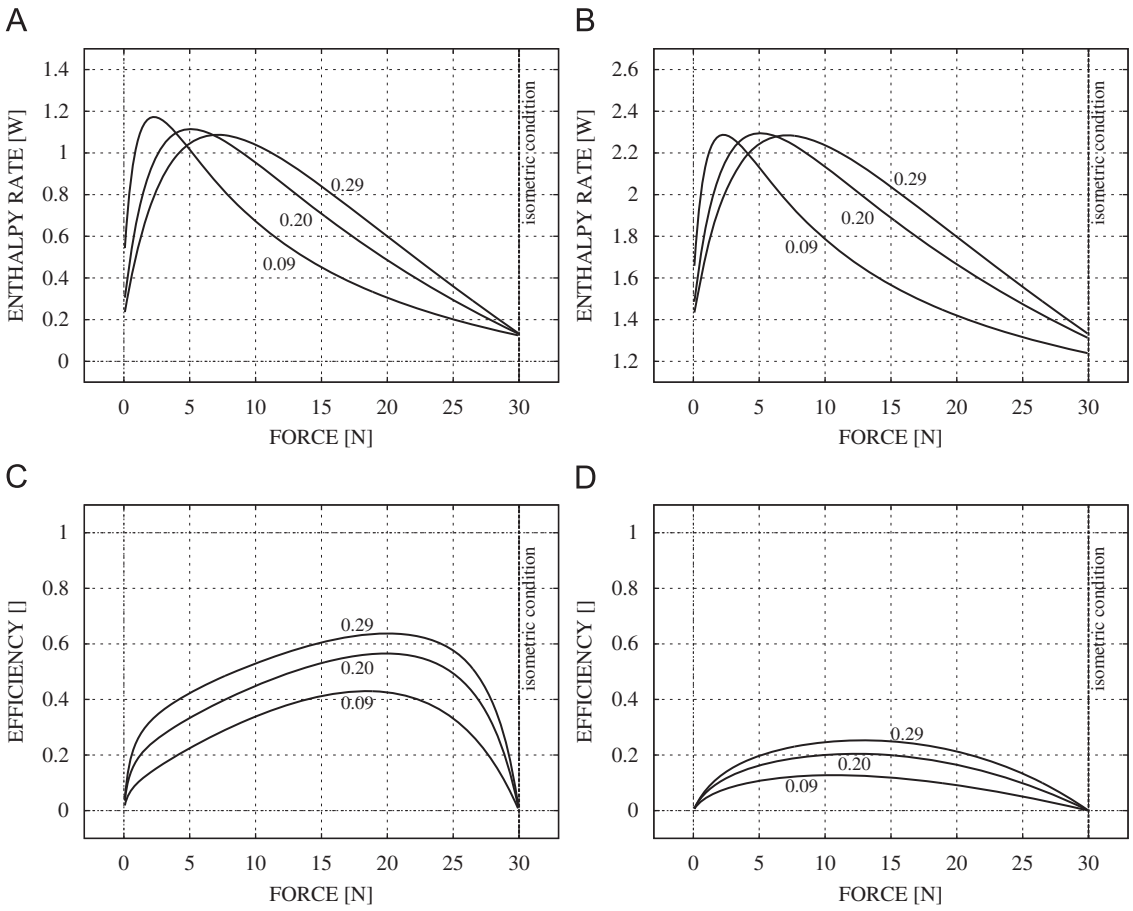

Fig. 3. Enthalpy rate $\dot{\mathcal{H}} = -F_M \cdot \dot{l}_M + \dot{h} + \dot{h}_0$ (top graphs A,B; note the different ordinate offset values) and mechanical efficiency $\varepsilon_M = -F_M \cdot \dot{l}_M / \dot{\mathcal{H}}$ (bottom graphs C,D) as functions of muscle force F_M for $F_{M,0} = F_{AE,max}$ with varied curvature of $\dot{l}_M(F_M)$, i.e. $\kappa_v \cdot D_{PDE,max} = const = 198\,\mathrm{N\,s/m}$ (labels $\kappa_v = 0.09, 0.20, 0.29$), and two coefficients $c_{\dot{h}_0}$ of maintenance heat rate $\dot{h}_0$, respectively (left graphs A,C: $c_{\dot{h}_0} = 0.03$ and right graphs B,D: $c_{\dot{h}_0} = 0.3$). Generally, $R_{PDE} = 0.01$ was chosen, therefore $\dot{h}_0$ (Eq. (22)) depends slightly on κ_v, along with $\dot{l}_{M,max}$ (Eq. (15)).

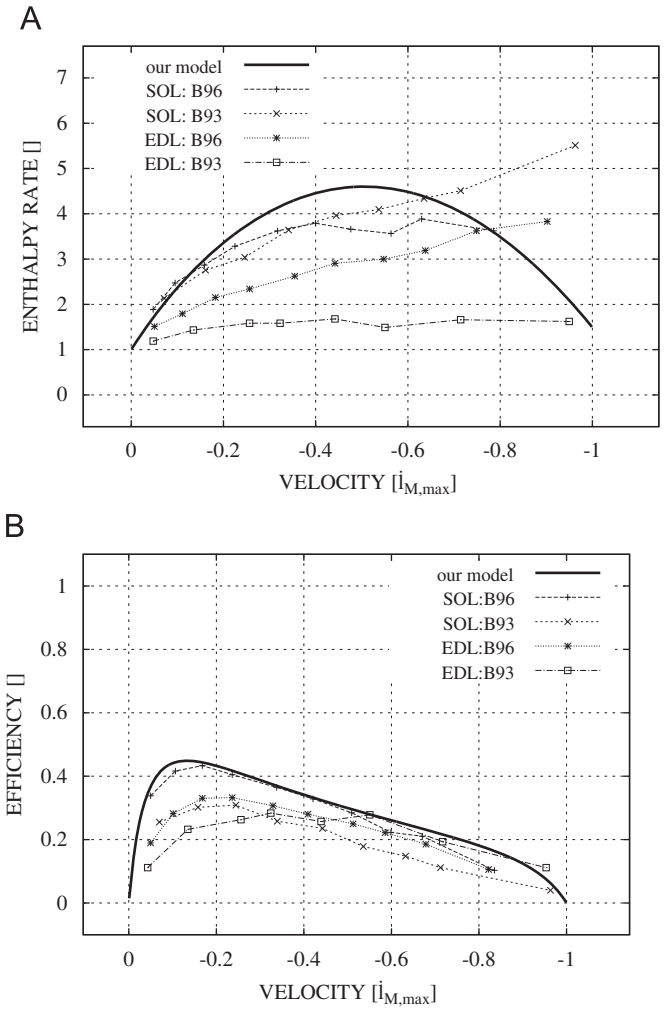

Fig. 4. Comparison of enthalpy rates (A, including maintenance heat rate, normalised to the latter) and mechanical efficiencies (B) from experiments (Barclay et al., 1993; Barclay, 1996) to those predicted by our model. The parameters of our model (identical to Fig. 2) represent a median piglet muscle (Günther et al., 2007): $F_{M,0}=F_{AE,max}=30\,\mathrm{N}$, $\kappa_v=0.20$, $D_{PDE,max}=1000\,\mathrm{N\,s/m}$ ($A_{rel}|_{R_{PDE}=0}=1/4$), $R_{PDE}=0.01$ ($\dot{l}_{M,max}=\dot{l}_{M,max}|_{R_{PDE}=0.01}=0.144\,\mathrm{m/s}$).

Section 3.2: $\kappa_v=0.09, 0.35$) of the net muscle power output during concentric contractions. The required mechanical energy must have been stored within the SE during the contraction history preceding the experimentally analysed contraction. In Appendix C we illustrate how our model can cover such storing situations that load the SE.

Note that the force contributions of AE and PDE always fight each other as the signs of F_{AE} and F_{PDE} are counter-directed. For themselves, they are usually distinctly higher than their net contribution $-F_M\cdot(1-\kappa_v)\cdot\dot{l}_M$. For instance, in case of $\kappa_v=0.09$ the SE power is 9% of net muscle power output. Here, exemplarily choosing a muscle velocity of $\dot{l}_M\approx-0.25\cdot\dot{l}_{M,max}$ with a belonging force $F_M\approx0.2\cdot F_{M,0}$, the power produced by the AE itself is $F_{AE}/F_M\approx0.75/0.2=3.75$ times higher than net muscle power output. F_{AE} is always higher than F_M as a result of comparing Eqs. (6) and (7). Here, the SE contributes only about $9\%/3.75=2.4\%$ of current AE power to net muscle power output. With $\dot{l}_{M,max}$ kept constant, in a less curved case of $\kappa_v=0.2$ (Hill, 1938) the SE would contribute approximately 10% of AE power to net muscle power output when contracting at a moderate velocity of about $-\dot{l}_{M,max}/3$.

4. Discussion

We demonstrated that the empirically formulated concentric force–velocity relation $\dot{l}_M(F_M)$ (Hill, 1938) of an activated muscle can generally be derived from a simple structural arrangement fulfilling an independent equation: the respective internal force equilibrium of three force bearing elements (AE, PDE, SE). Isolated function and connective arrangement of these elements (Fig. 1) have been confirmed both on macroscopic and microscopic levels for many decades, again and again. Eventually, just two other specific assumptions had to be superimposed: (i) the damping coefficient of the PDE must depend linearly on the force produced by the muscle, which is the only non-linearity of the model, and (ii) the gearing ratio κ_v between contraction velocity of the solely modelled internal degree of freedom and the whole muscle has to be introduced as a parameter. With this reduced approach Hill's empirical hyperbolic muscular force-velocity relation (Hill, 1938, 1964) can be transformed to a macroscopic mechanical model of the muscle. The Hill parameters A and B immediately arise as functions of minimum four model parameters. Our approach provides us with a platform to discuss how both the force–velocity relation and the maintenance heat rate may originate from the same transparent, physiologically based parameters, yet, without explicitly modelling detailed microscopic processes for a start.

Our model is based on five parameters. Three of them, representing the energy drain PDE ($D_{PDE,max}, F_{AE,max}, R_{PDE}$), are of straight mechanical, thus transparent, character, with R_{PDE} being ancillary. The fourth, the active force F_{AE}, is more entangled, first of all, because it is formally connected to the isometric force $F_{M,0}$ by an equation (Eq. (6)). Second, it conjoins all physiological processes of the muscular energy source, e.g. the dependency of the contractile machinery on sarcomere overlap and activation. The gearing ratio κ_v as a fifth parameter is, on the one hand, the most crucial for the force–velocity relation and, on the other hand, as pooling as F_{AE} and $F_{M,0}$, respectively. As proposed in Appendix A, we would interpret it as the clumped effect of stiffnesses and damping of AE, PDE, and SE. These transparent material properties determine the relative contribution κ_v of SE shortening to the current concentric contraction velocity of the muscle, and to the corresponding power output.

4.1. The gearing ratio κ_v: concentric contractions and maintenance heat rate

Originating in this conjoining character of κ_v, our model suggests a mechanism behind an observation as empirical and as old (Hill, 1938) as the Hill relation itself: the product $A\cdot B$ of the Hill parameters is assumed to equate, or at least to be in proportion to, the maintenance heat rate $\dot{h}_0$ (compare Section 3.2). Now, our model provides one possible causal explanation for that. For the parameter κ_v does not only shape all parameters of the Hill relation (Eqs. (16)–(18)) but also scales the maintenance heat rate $\dot{h}_0$ in proportion to the square of the ratio $\kappa_v/(1-\kappa_v)$ (Eqs. (22) and (23)), i.e. of the ratio between SE velocity and AE, PDE velocity. Remember that we also find $\kappa_v/(1-\kappa_v)=A_{rel}=A/F_{M,0}$ (Eq. (16)). Therefore, we suggest that both maintenance heat rate and all parameters of the Hill relation (Eqs. (16)–(18)) may be traced back directly to the same set of four parameters, with κ_v constituting a crucial one.

Former studies (Baker and Thomas, 2000; Pate et al., 1993; Woledge, 1968) have already suggested that interactions among crossbridges compromise overall work output. Treating the muscle as a thermodynamic instead of a mechanical system, Baker and Thomas (2000) found additionally that one specific

characteristic of muscular damping leads exactly to the Hill relation: dissipation should be force-dependent. Crossbridge interaction, i.e. some myosin heads stroking concentrically against other attached crossbridges loaded eccentrically, is also present in the isometric condition, which can be concluded from two studies (Daniel et al., 1998; Pate and Cooke, 1991).

In the Pate and Cooke (1991) study the interaction between a half-sarcomere and a microscopic force sensor made of an elastic needle in series was simulated. The authors aimed at the *sensor compliance* to be optimised within an experimental setup in order to measure sensitively rather than to suppress (“elastic damping”) the fluctuation amplitudes of the microscopic processes that occur within a real sarcomere. They described the interaction between a half-sarcomere and serial elasticity, the latter connected to a fixed point, as follows: any sudden stochastic change in the number of attached crossbridges, i.e. the pulling force of the half-sarcomere, requires a belonging adjustment in the *length* of the serial elastic needle. In turn, all remaining attached crossbridges will respond on their part by a displacement being partly concentric and partly eccentric. These permanent, stochastic, small-amplitude *fluctuations* are always present causing heat losses, even in the isometric condition in which source and drain balance to zero mechanical power output.

In the Pate and Cooke (1991) paper the effect of serial elasticity was examined as a parameter *external* to the sarcomere. Physiologically based compliance *internal* to the sarcomere adds up from actin (Huxley et al., 1994; Kishino and Yanagida, 1988; Wakabayashi et al., 1994), myosin (Huxley et al., 1994; Neumann et al., 1998; Wakabayashi et al., 1994), crossbridge (Ford et al., 1981; Goldman and Huxley, 1994; Huxley and Tideswell, 1996), and titin (Maruyama et al., 1977) connecting Z-disc and M-line. Using actin somehow as a representative for all these structures, the Daniel et al. (1998) study modelled the effect of internal serial compliance, distributed along the actin, on interactions among crossbridges. Amongst others, they could quantitatively reproduce two findings from experiments: force responses to rapid short range changes in length (Piazzesi et al., 1997; Seow et al., 1997) and inflections in the force–velocity relation at low shortening velocities (Edman et al., 1976). Serial compliance is the crucial factor for both findings.

In our model, the coupling of muscle force production to internal serial compliance is mapped in the simplest possible way: one internal degree of freedom resolved by one macroscopic parameter κ_v. Comparing our model to the situation within the Pate and Cooke (1991) study, the AE replaces the half-sarcomere and the SE replaces the needle. And in comparison to the Daniel et al. (1998) study, the AE maps the net work generation of crossbridges, whereas the SE maps net muscle internal serial compliance, whether it comes from actin, crossbridges, or other visco-elasticities within a sarcomere.

According to our estimate, net serial compliance would contribute about $10,\ldots,30\%$ to sarcomere length changes per time and, as compared to AE power, a $2.5,\ldots,10\%$ share in net mechanical power output during quasi-stationary concentric contractions. Thereby, the SE transmits any change in force to a change in length, and vice versa, of all crossbridges within a sarcomere and of other sarcomeres in series. From this point of view, therefore, the SE is not just a force transmitter but also an integral catalytic converter generating the macroscopic energy drain PDE by mechanically feeding back any crossbridge work stroke to other crossbridges. As a consequence, our model backs the view that the mechanics of concentric contractions and the origin of maintenance heat rate are indeed due to the same process (Huxley, 1957). Note, that this feedback character of the SE reappears in items (i: $d_{PDE}(F_M)$) *and* (ii: κ_v) crucial for the Hill relation. Up to now we have suggested a qualitative explanation for item (ii). According to item (i), the specific damping coefficient d_{PDE} depends on muscle force output F_M. However, as F_M *always equates the force* F_{SE} *in the SE* (Eq. (2)), the damping coefficient may also be symbolised by $d_{PDE}(F_{SE})$ (compare Eq. (4)). Furthermore, damping in proportion to muscle force may not only be qualitatively representative of stochastic feedback but also quantitatively representative of heat power release assumed to run approximately in proportion to the number of attached crossbridges doing work and, thus, releasing heat. Therefore, our model analysis based on the gearing ratio κ_v may help to connect Hill's, 1938 heat measurements, Huxley's (1957) sliding filament theory with a “stiffness” parameter k transforming crossbridge distribution to force output, modern compliant Huxley-type models (Daniel et al., 1998), and a more recent micro-mechanical muscle model (Denoth et al., 2002; Telley and Denoth, 2007).

In Sections 3.1 and 3.2 we had indirectly inferred realistic κ_v values from literature data on Hill parameters. Two recent studies (Barclay and Lichtwark, 2007; Loram et al., 2007) allow for more direct estimates from measuring finite shortening steps. At first, Barclay and Lichtwark (2007) determined the serial elasticity of a mouse muscle. Afterwards, they measured the forces during isovelocity contractions. Knowing the serial stiffness value from the first step, they calculated the relative velocity contribution of their hypothesised serial element. During initial 50 ms of an isovelocity contraction (compare Fig. 5 in Barclay and Lichtwark, 2007), a ratio $\dot{l}_{AE}:\dot{l}_{SE}\approx 2:5$, and therefore $\kappa_v\approx 0.7$, can be estimated (see Appendix A). This would be in striking contradiction to our prediction $\kappa_v\approx 0.2$ ($\dot{l}_{AE}:\dot{l}_{SE}\approx 4:1$). However, two aspects should be taken into account.

First, the most compliant serial elastic contribution dominates the net outcome. In the aforementioned muscle preparations (Barclay and Lichtwark, 2007) the tendons were at least partially included. According to the κ_v estimation mentioned above, we conclude that their “serial elastic component” (SEC) was dominated by tendinous (external) material, thus, hiding an about $(4/1)/(2/5)=10$ times stiffer fibre (internal) SE. Interestingly, Barclay and Lichtwark (2007) calculated almost exactly the same numbers. They compared their data to the stiffness of crossbridges and contractile filaments (Piazzesi and Lombardi, 1995). Barclay and Lichtwark (2007) estimated that this internal SE should be about 13 times stiffer than their SEC stiffness. Thus, our prediction of a realistic mean value $\kappa_v\approx 0.2$ matches literature data (Piazzesi and Lombardi, 1995; Barclay and Lichtwark, 2007) to a high degree. Also consistently, another recent study (Loram et al., 2007) concluded from directly visualising macroscopic elongations of fibres and tendons that the ratio of internal (fibre) to external (tendon) stiffness may range from about 30 to 1, depending on the load and elongation amplitudes, with an average ratio of 12 in case of short elongations typical for quiet human stance.

Second, we would like to annotate that dissipative coefficients might significantly contribute to or even dominate the gearing ratio κ_v in particular contraction modes. That is, κ_v might even be more representative of a distribution between parallel and serial damping than of a stiffness distribution. Whether this might both be compatible with a hyperbolic force–velocity relation and allow for an improved prediction of the enthalpy rate could be verified by introducing a serial damping element (SDE) into the current model, which would also imply history effects.

4.2. Perspective

Our model might be seen as the most reduced mechanical muscle model to derive the hyperbolic Hill relation from a basic principle. To that, it starts from one equation (force equilibrium)

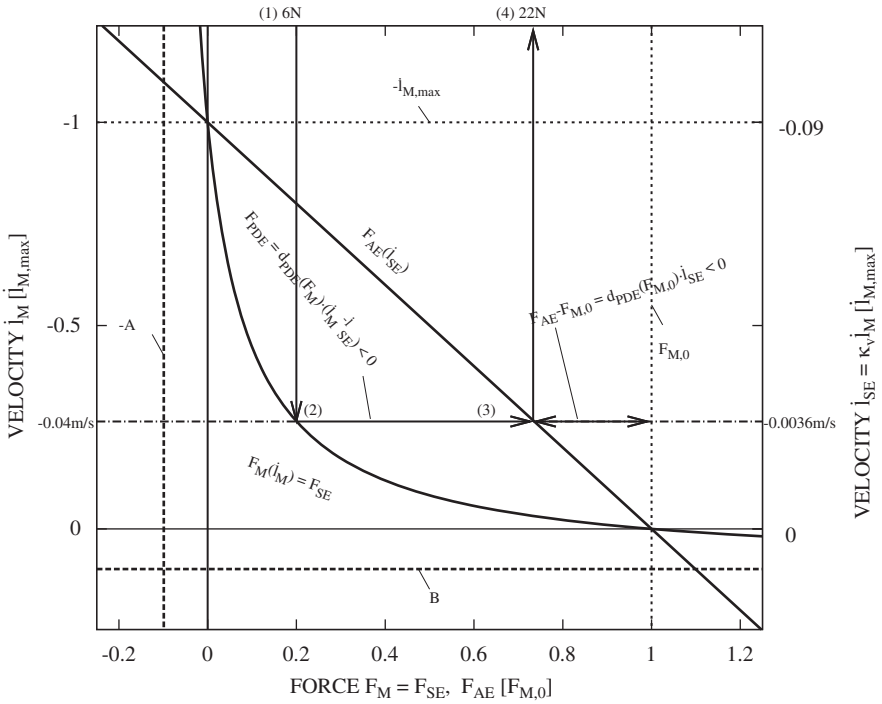

Fig. 5. Graphical representation of the force–velocity (Hill) relation Eq. (7) or Eq. (9), respectively, for an assumed gearing ratio $\kappa_v = 0.09$ between internal length l_{SE} and muscle length l_M contraction velocities $\dot{l}_{SE}$, $\dot{l}_M$ (Eq. (8)). A detailed explanation is given in Appendix B.

and requires minimally four mechanical parameters $F_{M,0}(q, l_M)$, $F_{AE,max}$, $D_{PDE,max}$, κ_v. Mathematically, the ratio $D_{PDE,max}/F_{AE,max}$ is actually relevant, i.e. just those three independent parameters that are necessary to uniquely determine a hyperbola would appear within our model.

It is not surprising that there are deviations between this extremely reduced model and real muscle. First, there is a discrepancy between our enthalpy–velocity relation and those from experiments, particularly at higher velocities. Second, there are deviations of the real muscle from a force–velocity hyperbola at high contraction velocities nearby $\dot{l}_{M,max}$ (Claflin and Faulkner, 1985; Julian et al., 1986; Reggiani, 2007) which are, however, difficult to discern experimentally. Third, there are indications that the force–velocity relation may generally be described by functions other than the hyperbolic Hill relation (see for example Abbott and Wilkie, 1953; Edman et al., 1976, 1978, 1997; Edman, 1988; Fenn and Marsh, 1935; Guschlbauer et al., 2007). In particular, Edman and co-workers highlighted repeatedly that the concentric force–velocity relation of real skeletal muscle deviates from one overall hyperbola at forces nearby the isometric condition $F_M > 0.8F_{M,0}$ (Edman et al., 1997). There and later (Daniel et al., 1998), a microscopic Huxley-type model, rather than a Hill-type model, was used. This might be the better choice for trying to calculate model responses that are meant to reproduce the fine structure of the force–velocity relation.

The deficient prediction of enthalpy rate at high velocities is a crucial challenge. For this purpose, PDE dependency on whole muscle force should be scrutinised: should we not rather conceive a dependency on F_{AE}, i.e. on the number of active crossbridges rather than on net muscle output force F_M? For a clear discrepancy between our prediction and measurements of enthalpy rate occurs when approaching maximum shortening velocity $\dot{l}_{M,max}$ at which F_M vanishes, but F_{AE} does not vanish at all. Next, we neglected the significant contribution (Barclay et al., 2007; Houdijk et al., 2006) of activation heat from Ca^{2+}–flux through the sarcoplasmatic reticulum to enthalpy rate. Though, as it depends on the rate of action potentials rather than on the number of active crossbridges, it might be treated in the simplest way by adding another heat rate parameter to the enthalpy rate (Eq. (20)). This would generally result in an about one third reduction of predicted relative enthalpy and in a slight decrease in efficiency (compare second paragraph of Section 3.2).

We developed our model for two reasons. First, we aimed at more insight into the basic mechanics behind macroscopic muscle contraction represented by the Hill relation. Second, the model was supposed to be bi-directional and to be as reduced as possible in order to be maximally transparent and feasible. Due to its bi-directional character caused by its derivation from force equilibrium, any structure of the muscle–tendon complex (e.g. serial and parallel elasticity, serial damping, tendon, aponeurosis) can be incorporated or coupled to the model transparently and explicitly as a force law. Therefore, as a predictive model it forms an extensible basis for modelling the active muscle in more detail. Furthermore, bi-directionality allows for coupling the muscle model to external dynamics, thus, using it in direct dynamic computer simulations.

Acknowledgements

Preparation of the manuscript accompanied us all through the year 2007 during which MG initially was supported by the "Deutsche Forschungsgemeinschaft" (DFG) Grant MU1766/1-2, in 2008 and 2009 by Grant MU1766/1-3. M.G. almost completely contributed at various places in Jena, Germany. There, he thanks André Seyfarth who really helped in rough seas during elapsing 2007. S.S. would like to thank the German Research Foundation (DFG) for financial support of the project within the Cluster of Excellence in Simulation Technology (EXC 310/1) at the University of Stuttgart. We are very grateful to Tobias Siebert, Christian Rode, Olaf Till, and Reinhard Blickhan in Jena for an invaluably inspiring discussion giving the manuscript a decisive

push. Even more, many thanks to Reinhard for a most attentive and committed reading of early manuscript drafts, for asking vital questions, and giving extremely incisive hints, again and again, during the whole preparation of this manuscript. Finally, M.G. cordially thanks all those creating the "Bohème" spirit that can turn work into purest joy. Above all, Mona and Lena may be awarded forevermore. Last but not least, atmosphere exuded by Evi and the subsequent charming lot at "Fairtrade Kontor" are, and will be, esteemed. Jessie, you did a really good job.

Appendix A. The gearing ratio κ_v as a function of material properties

The gearing ratio κ_v (Eq. (8)) can be calculated by modelling specific contraction situations. If, e.g., we arranged two elastic elements in series the contraction velocity of the serial arrangement would be distributed according to the stiffnesses of the elements. Thus, if all damping forces were neglected in the force equilibrium of Eq. (2) it would write $F_{SE} \approx F_{AE}$. Applying the first time derivative to this approximative force equilibrium, assuming the forces borne by all elements to depend on their respective lengths (F_{AE} on filament overlap and additionally on the muscle activation q), and using the chain rule we get

$$\frac{\partial F_{SE}(l_{SE})}{\partial l_{SE}} \cdot \dot{l}_{SE} = \frac{\partial F_{AE}(l_{AE}, q)}{\partial l_{AE}} \cdot \dot{l}_{AE} + \frac{\partial F_{AE}(l_{AE}, q)}{\partial q} \cdot \dot{q}. \tag{A.1}$$

After substituting $\dot{l}_{AE}$ from the time derivative of the kinematic equation $l_{AE} = l_M - l_{SE}$ into Eq. (A.1), further simplifying that the muscle activation q does not change (e.g. fully activated), and remembering the definition of κ_v (Eq. (8)) we find a specific gearing ratio

$$\kappa_v = \frac{\partial F_{AE}/\partial l_{AE}}{\partial F_{AE}/\partial l_{AE} + \partial F_{SE}/\partial l_{SE}}, \tag{A.2}$$

solely determined by elasticities, i.e. local stiffnesses of *AE* and *SE*.

However, this will only apply if the damping force in the PDE is clearly lower than the force in the AE due to its isometric force-length characteristic and elastic force also dominates in the SE. If, in contrast, the PDE term and damping in the SE became dominant and we further assumed that SE damping could be linearly approximated in proportion to its current contraction velocity the simplified force equilibrium $F_{SE} = d_{SE} \cdot \dot{l}_{SE} \approx d_{PDE} \cdot (\dot{l}_M - \dot{l}_{SE})$ would lead to

$$\kappa_v = \frac{d_{PDE}}{d_{PDE} + d_{SE}}, \tag{A.3}$$

the gearing ratio now solely determined by damping coefficients.

Finally and in general, we would expect κ_v to arise from the entirety of all elastic and dissipative muscle properties, i.e. to depend on the current lengths l_{AE}, l_{SE} plus the elastic and dissipative material parameters altogether determining the distribution of velocities $\dot{l}_{AE}$, $\dot{l}_{SE}$. Analogously, a very recent micro-mechanical muscle model (Denoth et al., 2002; Telley and Denoth, 2007) essentially derives the contraction dynamics of macroscopic muscle from coupling an in-series assembly of elementary force generating units mechanically, including inherent parallel and serial visco-elasticity.

Appendix B. Eqs. (7) and (9) as a sketch (Fig. 5)

The current muscle force F_M is the sum of three terms in Eq. (7). The first two terms equal the current AE force F_{AE} which is, in turn, $F_{M,0}$ plus a linear function in $\dot{l}_{SE}$ (Eq. (6)). The current force in the SE is always $F_{SE} = F_M$ (see Eq. (2)) and its current velocity always $\dot{l}_{SE} = \kappa_v \cdot \dot{l}_M$ (Eq. (8)), with the $\dot{l}_M$ scale plotted on the left ordinate and the $\dot{l}_{SE}$ scale plotted on the right ordinate. In Fig. 5 we used the parameter values $\kappa_v = 0.09$, $F_{AE,max} = F_{M,0} = 30\,\mathrm{N}$, $D_{PDE,max} = 2200\,\mathrm{N\,s/m}$, $R_{PDE} = 0$, thus, $\dot{l}_{M,max} = 0.152\,\mathrm{m/s}$, $A_{rel} = 0.1$.

In Fig. 5 the hyperbola $\dot{l}_M(F_M)$ is equivalently labelled by its inverse function $F_M(\dot{l}_M)$. In case of $R_{PDE} \neq 0$ the intersections of the straight line F_{AE} and the hyperbola $\dot{l}_M(F_M)$ with the force-axis separate due to

$$\dot{l}_{M,F_{AE}=0} = \frac{F_{AE,max}}{D_{PDE,max} \cdot \kappa_v} \cdot \frac{F_{M,0}}{(1-R_{PDE}) \cdot F_{M,0} + R_{PDE} \cdot F_{AE,max}} \neq \dot{l}_{M,max}$$

(compare Eq. (15)). The maximum contraction velocity of the muscle $\dot{l}_{M,max}$ is much more sensitive to $R_{PDE} > 0$ than $\dot{l}_{M,F_{AE}=0}$ is, with $\dot{l}_{M,max} < \dot{l}_{M,F_{AE}=0}$.

Following the path of the depicted arrows in Fig. 5 may help to gain an idea of the concentric contractile output of the muscle model elements SE, AE, PDE in an exemplary situation in which the muscle produces a force $F_M = F_{SE} = 6\,N$ (top label (1)). On the $\dot{l}_M$ scale to the left of label (2) we find its contraction velocity $\dot{l}_M = -0.04\,\mathrm{m/s}$. In the reverse case, currently requiring this velocity the muscle would provide the respective force due to the force – velocity relation being bi-directional. In the exemplary loading situation the SE contracts with the associated internal velocity $\dot{l}_{SE} = \kappa_v \cdot \dot{l}_M = -0.0036\,\mathrm{m/s}$ ($\dot{l}_{SE}$ scale to the right of label (3)). Eq. (6) constitutes the force $F_{AE}(\dot{l}_{SE})$ as a straight line in this diagram. It provides the current force output (see top label (4): $F_{AE} = 22\,\mathrm{N}$) of the AE.

The resulting asymptotes *A*, *B* (Hill parameters, see Eqs. (13) and (14)) and maximum contraction velocity $-\dot{l}_{M,max}$ (Eq. (15)) are also depicted. Length and activation dependency of F_{AE} reflect the chosen isometric force $F_{M,0}$ and vice versa (Eq. (6)). The difference between F_{AE} and $F_{M,0}$ (Eq. (6)) is depicted by the two-headed arrow to the right of label (3). The force in the PDE is the difference between current values of F_{AE} and $F_M(\dot{l}_M)$ (arrow between labels (2) and (3); see also Eqs. (2), (6), and (7)).

Appendix C. Internal redistributions in general: loading and unloading the SE by variation of F_{AE}

Eq. (6) generally describes the relation between active and isometric force. Eq. (6) also says that in the isometric case $\dot{l}_{SE}$ simply depends on the difference between active force $F_{AE}(q, l_M, l_{SE})$ and the current load of the muscle $F_M = F_{M,0} = F_{SE}(l_{SE})$. For $F_{AE} > F_M$ the SE is loaded ($\dot{l}_{SE} > 0$), for $F_{AE} < F_M$ the SE is unloaded ($\dot{l}_{SE} < 0$). Finally, if we abandon the isometric condition we find

$$\dot{l}_{SE} = \dot{l}_M + \frac{F_{AE}(q, l_M, l_{SE}) - F_{SE}(l_{SE})}{d_{PDE}(F_{SE}(l_{SE}))} \tag{C.1}$$

according to (Eq. (2)). Therefore, in case of calculating the internal length change for given muscle kinematics (e.g. isokinetic), $\dot{l}_M \neq 0$ would be just an additional term (compared to the isometric condition characterised by Eq. (6)) due to the assumption that the load is always applied to the active part of the muscle (AE and PDE) via a serial (visco-elastic) element with known characteristics.

References

Abbott, B.C., Wilkie, D.R., 1953. The relation between velocity of shortening and the tension-length curve of skeletal muscle. The Journal of Physiology 120 (1–2), 214–223.

Baker, J.E., Thomas, D.D., 2000. A thermodynamic muscle model and a chemical basis for A.V. Hill's muscle equation. Journal of Muscle Research and Cell Motility 1 (4), 335–344.

Barclay, C.J., 1994. Mechanical efficiency of fast- and slow-twitch muscles of the mouse performing cyclic contractions. The Journal of Experimental Biology 193 (Pt 1), 65–78.

Barclay, C.J., 1996. Mechanical efficiency and fatigue of fast and slow muscles of the mouse. The Journal of Physiology 497 (Pt 3), 781–794.
Barclay, C.J., 1999. A weakly coupled version of the Huxley crossbridge model can simulate energetics of amphibian and mammalian skeletal muscle. Journal of Muscle Research and Cell Motility 20 (2), 163–176.
Barclay, C.J., Constable, J.K., Gibbs, C.L., 1993. Energetics of fast- and slow-twitch muscles of the mouse. The Journal of Physiology 472, 61–80.
Barclay, C.J., Lichtwark, G.A., 2007. The mechanics of mouse skeletal muscle when shortening during relaxation. Journal of Biomechanics 40 (14), 3121–3129.
Barclay, C.J., Woledge, R.C., Curtin, N.A., 2007. Energy turnover for Ca^{2+} cycling in skeletal muscle. Journal of Muscle Research and Cell Motility 28 (4–5), 259–274.
Chin, L., Yue, P., Feng, J.J., Seow, C.Y., 2006. Mathematical simulation of muscle cross-bridge cycle and force–velocity relationship. Biophysical Journal 91 (10), 3653–3663.
Claflin, D.R., Faulkner, J.A., 1985. Shortening velocity extrapolated to zero load and unloaded shortening velocity of whole rat skeletal muscle. The Journal of Physiology 359, 357–363.
Cooke, R.H., White, H., Pate, E., 1994. A model of the release of myosin heads from actin in rapidly contracting muscle fibers. Biophysical Journal 66 (3 Pt 1), 778–788.
Curtin, N.A., Woledge, R.C., 1993. Efficiency of energy conversion during sinusoidal movement of white muscle fibres from the dogfish *Scyliorhinus canicula*. The Journal of Experimental Biology 183 (Pt 1), 137–147.
Daniel, T.L., Trimble, A.C., Chase, P.B., 1998. Compliant realignment of binding sites in muscle: transient behavior and mechanical tuning. Biophysical Journal 74 (4), 1611–1621.
Denoth, J., Stüssi, E., Csucs, G., Danuser, G., 2002. Single muscle fiber contraction is dictated by inter-sarcomere dynamics. Journal of Theoretical Biology 216 (1), 101–122.
Edman, K.A.P., 1988. Double-hyperbolic force-velocity relation in frog muscle fibres. The Journal of Physiology 404, 301–321.
Edman, K.A.P., Elzinga, G., Noble, M.I.M., 1978. Enhancement of mechanical performance by stretch during tetanal contractions of vertebrate skeletal muscle fibres. The Journal of Physiology 281, 139–155.
Edman, K.A.P., Månsson, A., Capuot, C., 1997. The biphasic force–velocity relationship in frog muscle fibres and its evaluation in terms of cross-bridge function. The Journal of Physiology 503 (1), 141–156.
Edman, K.A.P., Mulieri, L.A., Scubon-Mulieri, B., 1976. Non-hyperbolic force–velocity relationship in single muscle fibre. Acta Physiologica Scandinavica 98 (2), 143–156.
Elzinga, G., Lännergren, J., Stienen, G.J., 1987. Stable maintenance heat rate and contractile properties of different single muscle fibres from *Xenopus laevis* at 20°C. The Journal of Physiology 393, 399–412.
Fenn, W.O., Marsh, B.S., 1935. Muscular force at different speeds of shortening. The Journal of Physiology 85, 277–297.
Ford, L.E., Huxley, A.F., Simmons, R.M., 1981. The relation between stiffness and filament overlap in stimulated frog muscle fibres. The Journal of Physiology 311, 219–249.
Gasser, H.S., Hill, A.V., 1924. The dynamics of muscular contraction. Proceedings of the Royal Society of London B 96, 398–437.
Goldman, Y.E., Huxley, A.F., 1994. Actin compliance: are you pulling my chain? Biophysical Journal 67 (6), 2131–2133.
Günther, M., Ruder, H., 2003. Synthesis of two-dimensional human walking: a test of the λ−model. Biological Cybernetics 89 (2), 89–106.
Günther, M., Schmitt, S., Wank, V., 2007. High-frequency oscillations as a consequence of neglected serial damping in Hill-type muscle models. Biological Cybernetics 97 (1), 63–79.
Guschlbauer, C., Scharstein, H., Büschges, A., 2007. The extensor tibiae muscle of the stick insect: biomechanical properties of an insect walking leg muscle. The Journal of Experimental Biology 210 (Pt 6), 1092–1108.
Hanson, J., Huxley, H.E., 1953. The structural basis of the cross-striations in muscle. Nature 172 (4377), 530–532.
Hartree, W., Hill, A.V., 1920. The thermoelastic properties of muscle. Philosophical Transactions of the Royal Society of London B 210, 153–173.
Hill, A.V., 1922. The maximum work and mechanical efficiency of human muscles, and their most economical speed. The Journal of Physiology 56, 19–41.
Hill, A.V., 1938. The heat of shortening and the dynamic constants of muscle. Proceedings of the Royal Society of London B 126, 136–195.
Hill, A.V., 1950. The series elastic component of muscle. Proceedings of the Royal Society of London B 137, 273–280.
Hill, A.V., 1964. The effect of load on the heat of shortening of muscle. Proceedings of the Royal Society of London B 159, 1297–1318.
Hill, A.V., 1970. First and Last Experiments in Muscle Mechanics. Cambridge University Press, Cambridge.
Houdijk, H., Bobbert, M.F., de Haan, A., 2006. Evaluation of a Hill based muscle model for the energy cost and efficiency of muscular contraction. Journal of Biomechanics 39 (3), 536–543.
Huxley, A.F., 1957. Muscle structure and theories of contraction. Progress in Biophysics and Biophysical Chemistry 7, 255–318.
Huxley, A.F., 1973. A note suggesting that the cross-bridge attachment during muscle contraction may take place in two stages. Proceedings of the Royal Society of London B 183, 83–86.
Huxley, A.F., 2000. Mechanics and models of the myosin motor. Philosophical Transactions of the Royal Society of London B 355 (1396), 433–440.
Huxley, A.F., Niedergerke, R., 1953. Structural changes in muscle during contraction. Interference microscopy of living muscle fibres. Nature 173 (4412), 971–973.
Huxley, A.F., Tideswell, S., 1996. Filament compliance and tension transients in muscle. Journal of Muscle Research and Cell Motility 17 (4), 507–511.
Huxley, H.E., 2004. Fifty years of muscle and the sliding filament hypothesis. European Journal of Biochemistry 271 (8), 1405–1415.
Huxley, H.E., 2008. Memories of early work on muscle contraction and regulation in the 1950s and 1960s. Biochemical and Biophysical Research Communications 369 (1), 34–42.
Huxley, H.E., Hanson, J., 1954. Changes in the cross-striations of muscle during contraction and stretch and their structural interpretation. Nature 173 (4412), 973–976.
Huxley, H.E., Stewart, A., Sosa, H., Irving, T., 1994. X-ray diffraction measurements of the extensibility of actin and myosin filaments in contracting muscle. Biophysical Journal 67 (6), 2411–2421.
Julian, F.J., Rome, L.C., Stephenson, D.G., Striz, S., 1986. The maximum speed of shortening in living and skinned frog muscle fibres. The Journal of Physiology 370, 181–199.
Katz, B., 1939. The relation between force and speed in muscular contraction. The Journal of Physiology 96, 45–64.
Kishino, A., Yanagida, T., 1988. Force measurements by micromanipulation of a single actin filament by glass needles. Nature 334 (6177), 74–76.
Kistemaker, D.A., van Soest, A.J., Bobbert, M.F., 2006. Is equilibrium point control feasible for fast goal-directed single-joint movements? Journal of Neurophysiology 95 (5), 2898–2912.
Krueger, J.W., Pollack, G.H., 1975. Myocardial sarcomere dynamics during isometric contraction. The Journal of Physiology 251 (3), 627–643.
Lan, G., Sun, S.X., 2005. Dynamics of myosin-driven skeletal muscle contraction: I. Steady-state force generation. Biophysical Journal 88 (6), 4107–4117.
Levin, A., Wyman, J., 1927. The viscous elastic properties of muscle. Proceedings of the Royal Society of London B 101, 218–243.
Lichtwark, G.A., Wilson, A.M., 2005. A modified Hill muscle model that predicts muscle power output and efficiency during sinusoidal length changes. The Journal of Experimental Biology 208 (Pt 15), 2831–2843.
Lindstedt, S.L., Reich, T.E., Keim, P., LaStayo, P.C., 2002. Do muscles function as adaptable locomotor springs? The Journal of Experimental Biology 205 (Pt 15), 2211–2216.
Loram, I.D., Maganaris, C.N., Lakie, M., 2007. The passive, human calf muscles in relation to standing: the short range stiffness lies in the contractile component. The Journal of Physiology 584 (2), 677–692.
Lupton, H., 1922. The relation between the external work produced and the time occupied in a single muscular contraction in man. The Journal of Physiology 57, 68–75.
Lupton, H., 1923. An analysis of the effects of speed on the mechanical efficiency of human muscular movement. The Journal of Physiology 57, 337–353.
Maruyama, K., Matsubara, S., Natori, R., Nonomura, Y., Kimura, S., Ohashi, K., Murakami, F., Handa, S., Eguchi, G., 1977. Connectin, an elastic protein of muscle: characterization and function. Journal of Biochemistry 82 (2), 317–337.
McMahon, T.A., 1984. Muscles, Reflexes, and Locomotion. Princeton University Press, Princeton, NJ.
Minajeva, A., Kulke, M., Fernandez, J.M., Linke, W.A., 2001. Unfolding of titin domains explains the viscoelastic behavior of skeletal myofibrils. Biophysical Journal 80 (3), 1442–1451.
Neumann, T., Fauver, M., Pollack, G.H., 1998. Elastic properties of isolated thick filaments measured by nanofabricated cantilevers. Biophysical Journal 75 (2), 938–947.
Pandy, M.G., Zajac, F.E., Sim, E., Levine, W.S., 1990. An optimal control model for maximum height human jumping. Journal of Biomechanics 23 (12), 1185–1198.
Pate, E., Cooke, R., 1991. Simulation of stochastic processes in motile crossbridge systems. Journal of Muscle Research and Cell Motility 2 (4), 376–393.
Pate, E., White, H., Cooke, R., 1993. Determination of the myosin step size from mechanical and kinetic data. Proceedings of the National Academy of Sciences of the USA 90 (6), 2451–2455.
Piazzesi, G., Linari, M., Reconditi, M., Vanzi, F., Lombardi, V., 1997. Cross-bridge detachment and attachment following a step stretch imposed on active single frog muscle fibers. The Journal of Physiology 489, 3–15.
Piazzesi, G., Lombardi, V., 1995. A cross-bridge model that is able to explain mechanical and energetic properties of shortening muscle. Biophysical Journal 68 (5), 1966–1979.
Piazzesi, G., Lombardi, V., 1996. Simulation of the rapid regeneration of the actin–myosin working stroke with a tight coupling model of muscle contraction. Journal of Muscle Research and Cell Motility 17 (1), 45–53.
Reggiani, C., 2007. When fibres go slack and cross bridges are free to run: a brilliant method to study kinetic properties of acto-myosin interaction. The Journal of Physiology 583 (1), 5–7.
Seow, C.Y., Shroff, S.G., Ford, L.E., 1997. Detachment of low-force ridges contributes to the rapid tension transients of skinned rabbit skeletal muscle fibres. The Journal of Physiology 501, 149–164.
Telley, I.A., Denoth, J., 2007. Sarcomere dynamics during muscular contraction and their implications to muscle function. Journal of Muscle Research and Cell Motility 28 (1), 89–104.
van Soest, A.J., Bobbert, M.F., 1993. The contribution of muscle properties in the control of explosive movements. Biological Cybernetics 69 (3), 195–204.

Wakabayashi, K., Sugimoto, Y., Tanaka, H., Ueno, Y., Takezawa, Y., Amemiya, Y., 1994. X-ray diffraction evidence for the extensibility of actin and myosin filaments during muscle contraction. Biophysical Journal 67 (6), 2422–2435.

Wang, K., McCarter, R., Wright, J., Beverly, J., Ramirez-Mitchell, R., 1993. Viscoelasticity of the sarcomere matrix of skeletal muscles. The titin-myosin composite filament is a dual-stage molecular spring. Biophysical Journal 64 (4), 1161–1177.

Wank, V., Fischer, M.S., Walter, B., Bauer, R., 2006. Muscle growth and fiber type composition in hind limb muscles during postnatal development in pigs. Cells Tissues Organs 182 (3–4), 171–181.

Winters, J.M., 1990. Hill-based muscle models: a system engineering perspective. In: Winters, J.M., Woo, S.L. (Eds.), Multiple Muscle Systems. Springer, New York, pp. 69–93 (Chapter 5).

Woledge, R.C., 1968. The energetics of tortoise muscle. The Journal of Physiology 197 (3), 685–707.

Zajac, F.E., 1989. Muscle and tendon: properties, models, scaling, and application to biomechanics and motor control. In: Bourne, J.R. (Ed.), CRC Critical Reviews in Biomedical Engineering, vol. 17. CRC Press, Boca Raton, pp. 359–411.